Structure and Bonding of Bromoantimonate(III) Complexes with Unusual Valency by Means of NQR and Powder X-Ray Diffraction *

Tsutomu Okuda, Yoshihiro Kinoshita, Hiromitsu Terao **, and Koji Yamada

Department of Chemistry, Faculty of Science, Hiroshima University, Kagamiyama 1 Chome, Higashi-Hiroshima 724, Japan

Z. Naturforsch. **49a**, 185–192 (1994); received July 23, 1993

NQR and powder X-ray diffraction were observed for several bromoantimonate (III) complexes which contain $C_nH_{2n+1}NH_3$ ($n=1-3$) or $(C_nH_{2n+1})_2NH_2$ ($n=1-4$) as a cation. The bond character, anion structure, crystal structure, and phase transition are discussed on the basis of the three-center-four-electron bond. A good correlation was found between the halogen NQR frequency and the Sb-X bond length.

Key words: ^{81}Br NQR; Temperature dependence; Phase transition; Crystal structure.

Introduction

Halogenoantimonate(III) complexes are stereochemically interesting because anions of these complexes have various compositions and structures [1–3]. Despite the diversity of the anion structure, the coordination number about the central atom is generally six. In order to attain six-coordination, the central atoms are forced to form polymeric structures by association among them, resulting in the presence of various bond lengths. We observed NQR and X-ray diffraction for several bromoantimonate (III) complexes in order to examine the structure and bond character, the ionic motion, and the phase transition.

Experimental

The complexes were prepared by the following methods. (a) Sb_2O_3 was dissolved in concentrated hydrobromic acid and added to a small excess of alkylammonium hydrobromide which was prepared by adding a stoichiometric amount of concentrated hydrobromic acid to the alkylamine. The solution was heated and stirred till the amine hydrobromide was completely dissolved. Large crystals were obtained by slow recrystallization from the saturated solution which was placed together with sodium hydroxide in a vacuum desiccator. (b) Stoichiometric amounts of $SbBr_3$ and the amine hydrobromide were sealed in a glass tube and heated at about 380 K for 10 days in an electric furnace. All the complexes were identified by CHN elemental analysis as listed in Table 1.

NQR signals were observed by using super-regenerative spectrometers and a Matec pulsed spectrometer. The desired sample temperature was obtained by adding liquid nitrogen to liquid petroleum in a Dewar vessel. The X-ray diffraction patterns were obtained by the Rigaku Rad-B system. The Fortran program developed by Izumi was used for the Rietveld analysis [4].

Table 1. Chemical analysis of bromoantimonate(III) complexes.

Compound	Found (%)			Calculated (%)		
	C	H	N	C	H	N
$(C_2H_5NH_3)_2SbBr_5$	7.99	2.60	4.53	7.83	2.63	4.57
$(n\text{-}C_3H_7NH_3)_3SbBr_5$	11.62	3.14	4.37	11.23	3.14	4.37
$(CH_3NH_3)_3SbBr_6$	5.28	2.52	5.73	5.17	2.60	6.03
$[(CH_3)_2NH_2]_3SbBr_6$	9.61	3.13	5.65	9.75	3.27	5.68
$[(C_2H_5)_2NH_2]_3SbBr_6$	17.78	4.25	5.01	17.50	4.41	5.10
$[(n\text{-}C_3H_7)_2NH_2]_3SbBr_6$	24.01	5.40	4.57	23.82	5.33	4.63
$[(n\text{-}C_4H_9)_2NH_2]_3SbBr_6$	29.06	6.02	4.09	29.06	6.10	4.24

* Presented at the XIIth International Symposium on Nuclear Quadrupole Resonance, Zürich, July 19–23, 1993.

** Faculty of Integrated Arts and Science, Tokushima University Minamijosanjima-cho, Tokushima 770, Japan.

Reprint requests to Prof. T. Okuda, Department of Chemistry, Faculty of Science, Hiroshima University, Kagamiyama 1 Chome, Higashi-Hiroshima 724, Japan.

0932-0784 / 94 / 0100-0185 $ 01.30/0. – Please order a reprint rather than making your own copy

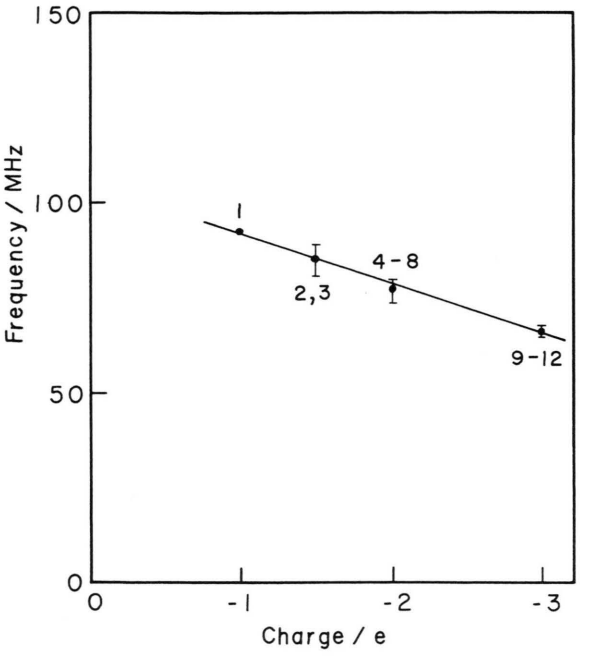

Fig. 1. Correlation between the ^{81}Br NQR frequency and the charge on the $SbBr_{3+n}^{n-}$ anion. 1, $(C_5H_4NH)SbBr_4$; 2, $(CH_3NH_3)_3Sb_2Br_9$; 3, $[(CH_4)N]_3Sb_2Br_9$; 4, $(CH_3NH_3)_3SbBr_6$; 5, $(C_2H_5NH_3)_2SbBr_5$; 6, $(n\text{-}C_3H_7NH_3)_2SbBr_5$; 7, $(C_6H_5NH_3)_2SbBr_5$; 8, $(4\text{-}CH_3C_5H_5NH)_2SbBr_5$; 9, $[(CH_3)_2NH_2]_3SbBr_6$; 10, $[C_2H_5)_2NH_2]_3SbBr_6$; 11, $[(n\text{-}C_3H_7)_2NH_2]_3SbBr_6$; 12, $[(n\text{-}C_4H_9)_2NH_2]_3SbBr_6$.

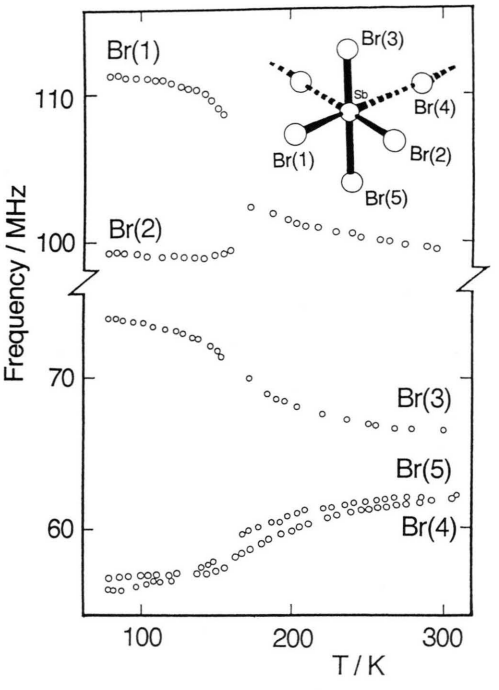

Fig. 2. Temperature dependence of ^{81}Br NQR frequencies in $(C_2H_5NH_3)_2SbBr_5$.

Table 2. ^{81}Br NQR frequencies of bromoantimonate(III) complexes at 77 K.

Compound	Frequencies/MHz			Mean frequency/MHz
$(CH_3NH_3)_3SbBr_6$	105.77	104.26	78.51	80.07
	61.22	50.58		
$(C_2H_5NH_3)_2SbBr_5$	111.33	99.34	74.02	79.50
	56.84	55.95		
$(n\text{-}C_3H_7NH_3)_2SbBr_5$	83.42	74.34	53.67	73.84
$[(CH_3)_2NH_2]_3SbBr_6$	68.73	67.21	64.91	65.69
	61.90			
$[(C_2H_5)_2NH_2]_3SbBr_6$	103.39	32.57		67.98
$[(n\text{-}C_3H_7)_2NH_2]_2SbBr_6$	65.40			65.40
$[(n\text{-}C_4H_9)_2NH_2]_3SbBr_6$	69.73	69.61	69.28	66.97
	68.77	68.45	68.24	
	67.76	67.04	65.59	
	63.93	62.78	62.42	

Results and Discussion

^{81}Br NQR spectra were observed for bromoantimonate (III) complexes. The NQR frequencies and the mean frequency are listed in Table 2. Taking into account the ^{35}Cl NQR spectra and their temperature dependence in $(C_6H_5NH_3)_2SbCl_5$ [5], the anions in $(C_2H_5HN_3)_2SbBr_5$ and $(n\text{-}C_3H_7NH_3)_2SbBr_5$ are considered to form infinite chains by bromine bridges with four terminal and two bridging Br atoms around the Sb atom in the anion.

Figure 1 shows the correlation between the mean ^{81}Br NQR frequency of the complex and the charge on the $SbBr_{3+n}^{n-}$ anion. The relation is expressed by

$$\nu(^{81}\mathrm{Br}) = (12.9\chi + 104.7)\ \mathrm{MHz}\,, \qquad (1)$$

where $\nu(^{81}\mathrm{Br})$ is the mean ^{81}Br NQR frequency and χ the charge on the anion in electronic units. The mean ^{81}Br NQR frequency in the $SbBr_5^{2-}$ anion is considerably higher than that in the $SbBr_6^{3-}$ anion, indicating that the ionic character of the Sb–Br bond is larger in the latter anion than in the former. Thus, the formal charge of the anion affects the Sb–Br bond character.

Figures 2 and 3 show the temperature dependences of the ^{81}Br NQR frequencies for $(C_2H_5NH_3)_2SbBr_5$ and $(CH_3NH_3)_3SbBr_6$, respectively. These tempera-

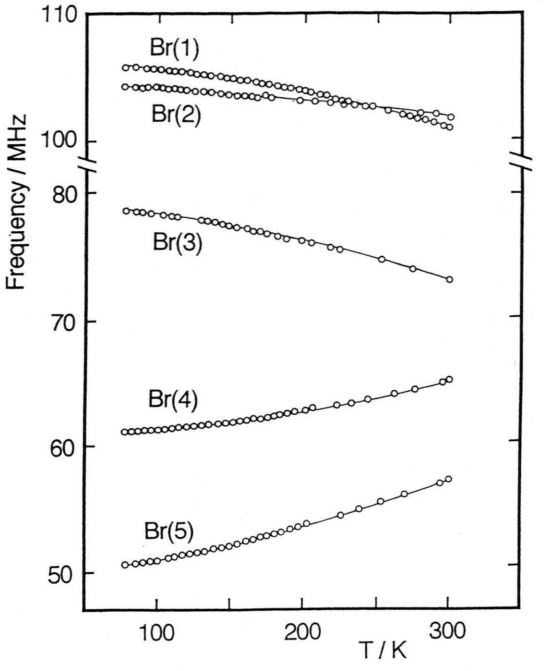

Fig. 3. Temperature dependence of ^{81}Br NQR frequencies in $(CH_3NH_3)_3SbBr_6$.

ture dependences resemble each other, i.e. with increasing temperature the three higher NQR frequencies decrease while the two lower ones increase. These features are similar to that of $[C_6H_5NH_3]_2SbCl_5$ but different from that of $[C_6H_5NH_3]_3SbCl_6$ [5] and suggest that the $SbBr_6$ fragment in $(CH_3NH_3)_3SbBr_6$ consists of a discrete Br^- anion and an $SbBr_5^{2-}$ anion which forms an infinite chain. This type of anion has already been found in $(CH_3NH_3)_3SbCl_6$ [6], but is quite rare, while discrete SbX_6^{3-} anions are well known [7, 8]. Our NQR results suggest that the complex with the $SbBr_5^{2-}$ anion tends to form when the cation is a primary ammonium while the complex with the $SbBr_6^{3-}$ anion tends to form when the cation is a secondary ammonium.

In order to confirm the anion structure, the powder X-ray diffraction was measured and its pattern was analysed by the Rietveld method. The Rietveld refinements were done by using dummy atom (K^+) instead of the $CH_3NH_3^+$ cations. Figure 4 shows the best-fit profiles together with the raw data. The crystallographic parameters and experimental details are listed in Table 3, the positional and thermal parameters in Table 4, and the bond lengths in Table 5. The crystal structure is shown in Figure 5. The complex contains

Table 3. Crystal data and experimental details of the Rietveld refinement of $(CH_3NH_3)_3SbBr_6$.

Temperature	293 K
Space group	$P2_1/c$
Crystal system	Monoclinic
Lattice constants	$a=13.577(1)$ Å, $b=8.254(1)$ Å, $c=21.665(2)$ Å, $\beta=134.05(1)°$
z	4
Number of parameters	57
2θ range	7°–67°
Step width	0.04°
R_p [a]	0.068
R_F [b]	0.033

[a] $R_p=\sum y_i(\text{obs})-y_i(\text{cal})/\sum y_i(\text{obs})$, where $y_i(\text{obs})$, $y_i(\text{cal})$ are the observed and calculated intensity at ith step.
[b] $R_F=\sum(I_K(\text{obs}))^{1/2}-(I_K(\text{cal}))^{1/2}/\sum I_K(\text{obs})^{1/2}$, where I_K is the intensity assigned to the Kth Bragg reflection.

Table 4. Positional and isotropic thermal parameters of $(CH_3NH_3)_3SbBr_6$ with standard deviations of the least significant figures in parentheses [a].

Atom	X	Y	Z	B_{ISO}/Å^2
Sb	0.3124(13)	0.3313(20)	0.2209 (8)	3.2 (4)
Br(1)	0.1488(18)	0.5817(28)	0.1764(11)	2.1 (7)
Br(2)	0.1811(17)	0.2949(26)	0.0548(10)	1.7 (6)
Br(3)	0.1606(17)	0.1106(27)	0.2183 (9)	1.2 (6)
Br(4)	0.4620(20)	0.4067(27)	0.4015(11)	3.7 (7)
Br(5)	0.4811(20)	0.5780(25)	0.2245(12)	2.2 (7)
Br(6)	0.8132(16)	0.3406(28)	0.1288(10)	1.6 (6)
$CH_3NH_3(1)$	0.890 (5)	−0.086 (7)	0.159 (3)	15.7(24)
$CH_3NH_3(2)$	0.450 (8)	0.876 (9)	0.417 (4)	29.5(32)
$CH_3NH_3(3)$	0.161 (6)	0.737 (9)	0.022 (4)	29.0(30)

[a] Dummy atom K^+ was used for the refinement instead of $CH_3NH_3^+$.

Table 5. Bond distances (Å) in $(CH_3NH_3)_3SbBr_6$.

Sb–Br(1)	2.675(23)	Br(6)–$CH_3NH_3(1)$	3.55(5)
Sb–Br(2)	2.700(19)	Br(6)–$CH_3NH_3(2)$	3.51(7)
Sb–Br(3)	2.723(24)	Br(6)–$CH_3NH_3(3)$	3.58(6)
Sb–Br(4)	2.963(21)	Br(6)–$CH_3NH_3(1)$ [b]	3.71(5)
Sb–Br(5)	3.024(24)		
Sb[a]–Br(5)[a]	3.003(24)		

[a] Symmetry code: $1-x$, $0.5+y$, $0.5-z$.
[b] Symmetry code: $2-x$, $0.5+y$, $0.5-z$.

the discrete Br^- anion which forms CH_3NH_3Br with the $CH_3NH_3^+$ cation and the $SbBr_5^{2-}$ anion which forms the chain structure by bromine bridges. This structure is consistent with our NQR results.

As Figure 2 shows, the two higher ^{81}Br resonance lines in $(C_2H_5NH_3)_2SbBr_5$ coalesce into one line and the temperature dependence of the remaining lines

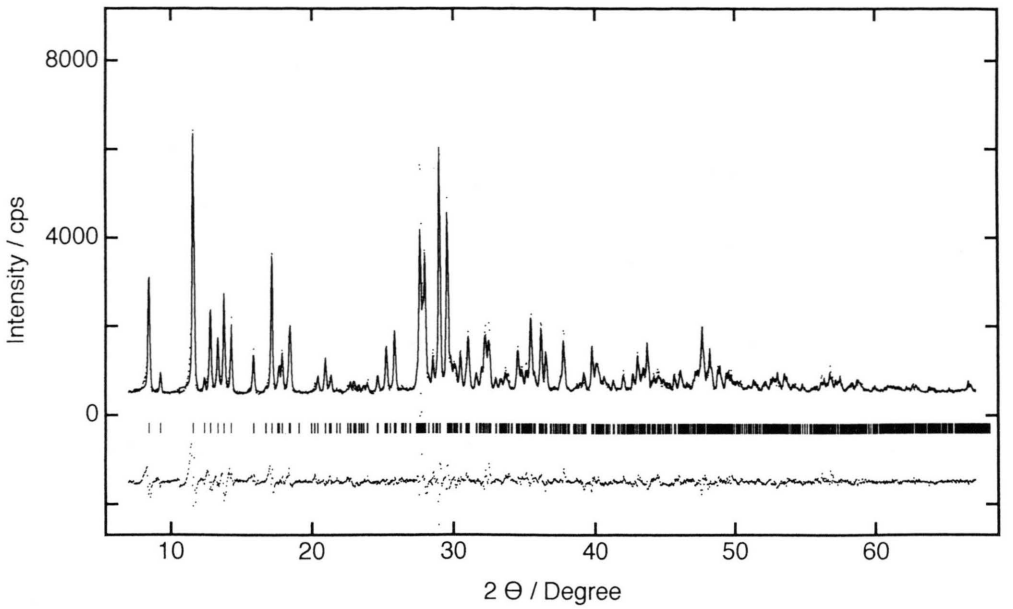

Fig. 4. Final results of the Rietveld refinements for $(CH_3NH_3)_3SbBr_6$. In the upper portion the observed data are shown by dots; the calculated patterns are given by the solid line. The lower parts are plots of the difference. The intensity is given in arbitrary unit.

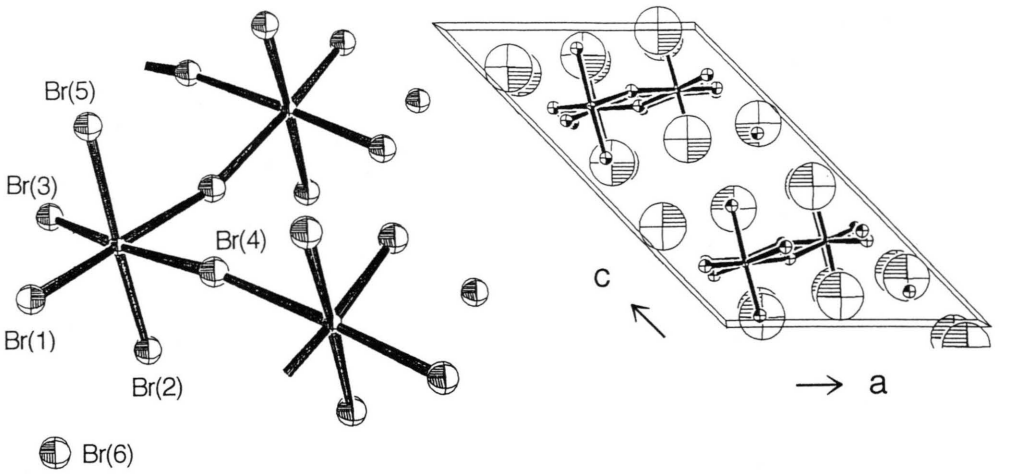

Fig. 5. Crystal structure of $(CH_3NH_3)_3SbBr_6$.

changes the slope at about 155 K, suggesting the presence of a phase transition. The DTA measurements were carried out in the temperature range of 77 K to 450 K. The results are shown in Figure 6. When the sample was cooled, one exothermic event was observed at 157.2 K. When the sample was heated, one endothermic event was observed at 155.1 K. The transition point is in good agreement with that from the NQR measurements.

In order to obtain further information about the phase transition, we observed the ^{81}Br NQR spin-lattice relaxation time for the second highest resonance line. The results are shown in Figure 7. When the temperature rose from 77 K, the relaxation time decreased gradually and then sharply from about 150 K onwards. The phase transition is responsible for the discontinuity near 160 K. ^{81}Br NQR spin-lattice relaxation time is assumed as the sum of contributions

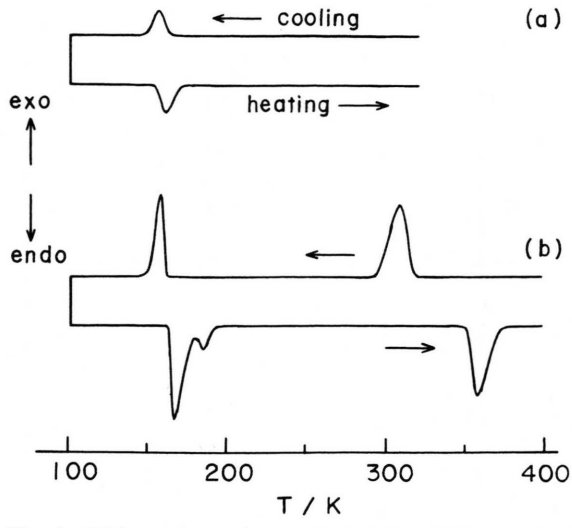

Fig. 6. DTA curves of (a) $(C_2H_5NH_3)_2SbBr_5$ and (b) $(n\text{-}C_3H_7NH_3)_2SbBr_5$.

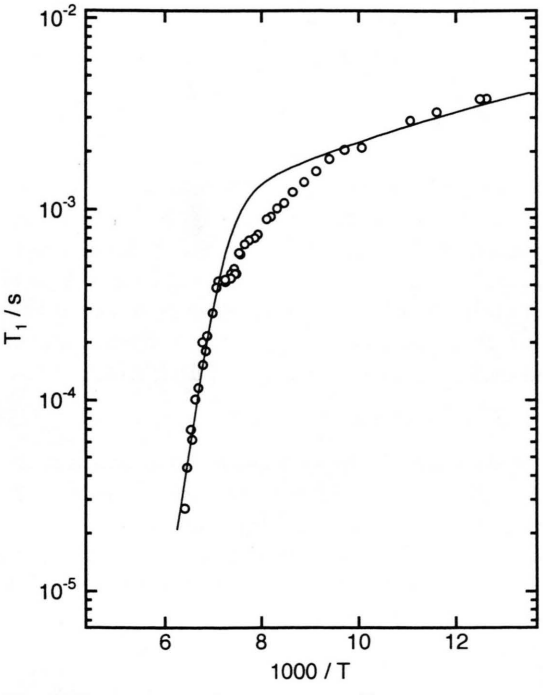

Fig. 7. Temperature dependence of ^{81}Br NQR spin-lattice relaxation time in $(C_2H_5NH_3)_2SbBr_5$.

from the libration of the cation as well as the complex anion, $(T_1)_{latt}$, the reorientation of the complex anion, $(T_1)_{reo}$, and the modulation of the bromine electric field gradient due to the reorientation of the cation, $(T_1)_{mod}$. Therefore, the observed temperature dependence of the relaxation time is expressed by the equation [9–11].

$$1/(T_1)_{obs} = 1/(T_1)_{latt} + 1/(T_1)_{mod} + 1/(T_1)_{reo}\,, \qquad (2)$$

where

$$1/(T_1)_{latt} = a\,T^2\,,$$
$$1/(T_1)_{reo} = b\exp(-E/RT)\,,$$
$$1/(T_1)_{mod} = (1/3\tau_0)\,(q'/q)^2\exp(-E/T)\,.$$

Here E, τ_0, and (q'/q) are the activation energy of the motion, the correlation time at infinite temperature, and the fluctuation fraction of the electric field gradient, respectively. In this complex the contribution from the reorientation of the anion may be ignored because the anions form the infinite chain.

By fitting (2) to the experimental T_1 values, we obtain

$$(T_1^{-1})_{obs} = 0.0449\,T^2 + 3.5\cdot 10^{15}\exp(-33.3/R\,T)\,.$$

The activation energy of the cationic motion is 33.3 kJ/mol. The cationic motions are considered to be the reorientation of the CH_3 and NH_3 groups around their C_3 axes and the motion of the ethylammonium group as a whole. The activation energy obtained is too large to be considered as resulting from the reorientation of the CH_3 group. The activation energy for the reorientation of the NH_3 group about the C_3 axis has been reported to be 25–28 kJ/mol in a few compounds [12, 13]. These values are comparable with that obtained in $(C_2H_5NH_3)_2SbBr_5$.

In order to obtain information on the motion of the cation, we measured ^1H NMR spectra at various temperatures. Figure 8 shows the temperature dependence of the second moments of the ^1H NMR line between 125 K and 290 K. With increasing temperature, the second moment decreased first gradually and then rapidly from about 150 K until it became 4.2 G^2 at 180 K. With a further increase in temperature, the second moment dropped gradually to 2.7 G^2 at 290 K. Since the value at 125 K is small, both the CH_3 and NH_3 groups are considered to be reorientating about their C_3 axes. Therefore, the rapid decrease near 150 K is considered to be due to the motion of the ethylammonium cation around its long axis as a whole.

For $(n\text{-}C_3H_7NH_3)_2SbBr_5$ we have already reported the temperature dependence of ^{81}Br NQR lines [3]. When the temperature rose from 77 K, the highest resonance frequency increased, the remaining frequencies decreased and all resonance lines disappeared at

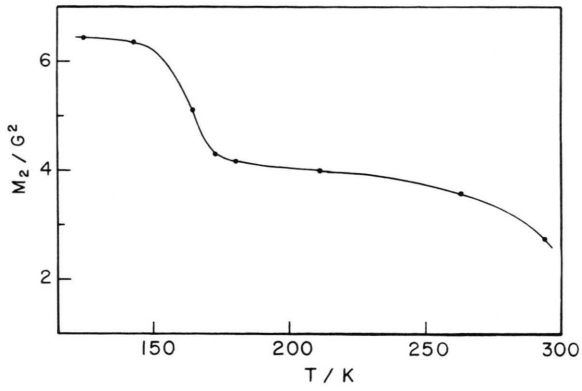

Fig. 8. Temperature dependence of the second moments (M_2) of the ^{1}H NMR line in $(C_2H_5NH_3)_2SbBr_5$.

about 160 K. With further increase in temperature up to room temperature, no NQR lines were observed. Figure 6 b shows the DTA curves of the complex. On cooling two exothermic peaks were observed at 331.9 K and 162.2 K, and on heating three endothermic peaks were observed at 164.0 K, 183.7 K, and 351.9 K. The two peaks appearing near 170 K during the heating run were too close to determine the starting point of the higher temperature anomaly. The DTA measurement suggests the presence of at least four solid phases.

Figure 9 shows the ^{81}Br NQR spin-lattice relaxation time for the middle line. With increasing temperature, the relaxation time decreased monotonously up to 150 K, and then the NQR signal disappeared. The phase transition is considered to be responsible for the disappearance of the resonance line. As expressed by (2), the spin-lattice relaxation time is proportional to T^{-2} when the relaxation mechanism is attributable to lattice vibrations. The experimental values could be approximated by $1/(T_1)_{obs} \propto T^4$. The reason for the large deviation of the temperature dependence of T_1 form T^{-2} is not known.

As listed in Table 2, the NQR frequencies of the complexes with the secondary ammonium cations lie in the region of 30 MHz to 105 MHz, the mean frequency being almost constant (65 MHz–68 MHz). The NQR results show that these complexes have a discrete octahedral $SbBr_6^{3-}$ anion., The powder X-ray diffraction patterns were obtained for the complexes with the secondary ammonium [14]. The results show that the Sb–Br bond lengths of these complexes range from 2.6 Å to 3.1 Å, suggesting the presence of interaction of the anion with the cation.

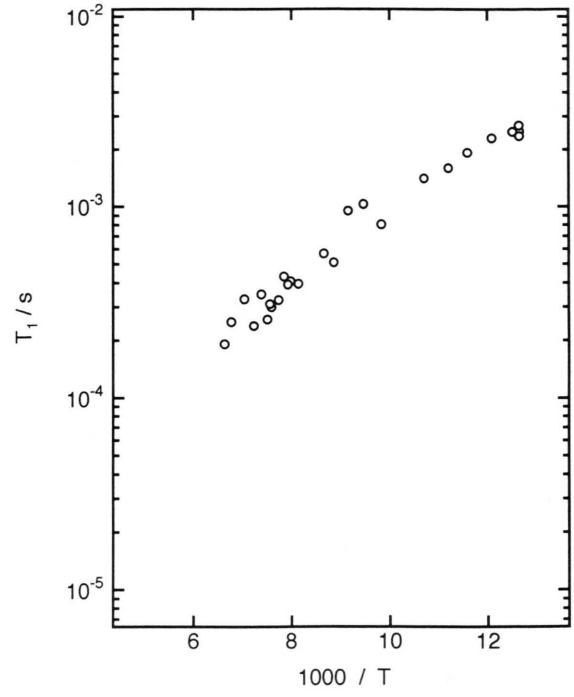

Fig. 9. Temperature dependence of ^{81}Br NQR spin-lattice relaxation time in $(n\text{-}C_3H_7NH_3)_2SbBr_5$.

In order to examine the bond character of the X–Sb · · · X bond which is formed by the three-center-four-electron (3c–4e) bond, the Sb–X bond length was plotted against the Sb · · · X bond length. A good correlation was found between them as shown in Figure 10. A relation between the bond length and the bond order has been derived by Pauling [15]:

$$d = d_0 - a \log n , \tag{3}$$

where d_0 is the length of a single bond and n is the bond order. In the halogenoantimonate(III) complexes, the Sb atom attains six-coordination, as mentioned above. Therefore each anion has three trans X–Sb · · · X bonds. In the trans bond, the two Sb–X bond lengths are expressed by

$$d_1 = d_0 - a \log n_1 ,$$
$$d_2 = d_0 - a \log n_2 ,$$

where d_1 and d_2 are the bond lengths of the Sb–X and Sb · · · X bonds, respectively and the sum of the bond order $(n_1 + n_2)$ is 1 for one trans X–Sb–X bond. Figure 10 shows the plot of d_2 against d_1 for halogenoantimonate(III) complexes. The figure indicates that when one Sb–Br bond in the trans bond is long, the other is short, and vice versa. The following parame-

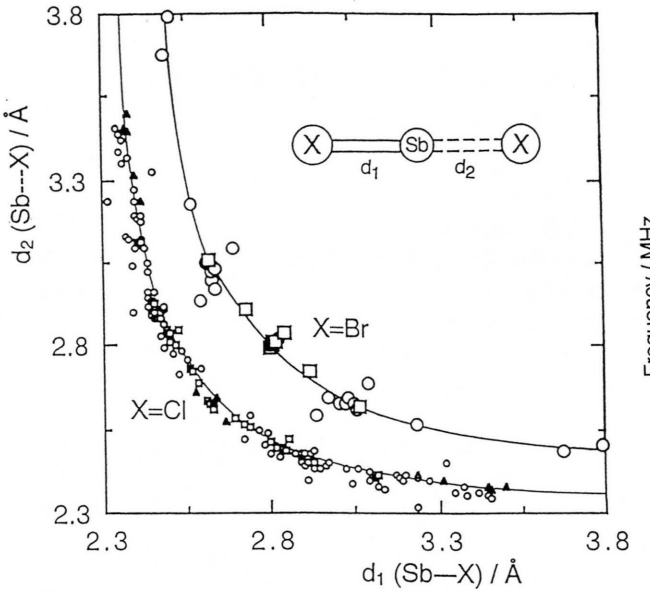

Fig. 10. Correlation between X–Sb and Sb · · · X bond lengths for halogenoantimonate(III) complexes. ▲: X(bridge)–Sb–X(bridge); ○: X(terminal)–Sb–X(bridge); □: X(terminal)–Sb–X(terminal).

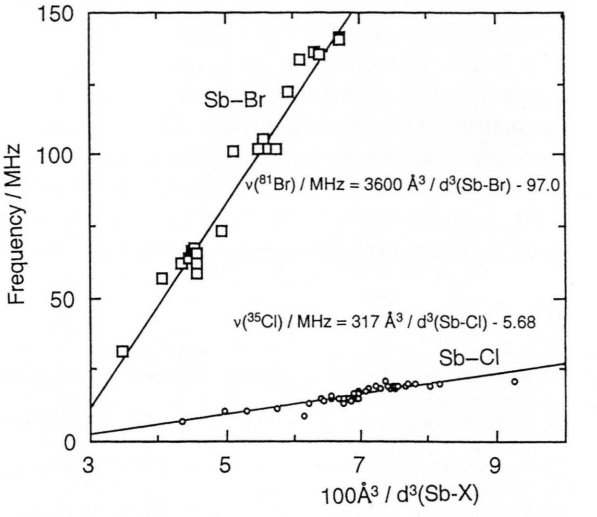

Fig. 12. Plot of NQR the frequency against minus the third power of the bond length.

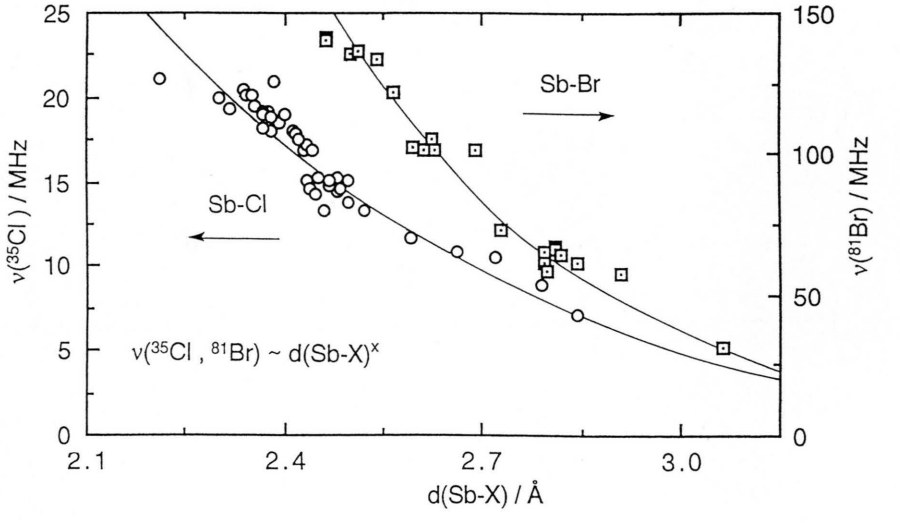

Fig. 11. Correlation between NQR frequency and Sb–X bond length.

ters were obtained: $d_0 = 2.34$ Å and $a = 1.00$ for the chlorides and $d_0 = 2.46$ Å and $a = 1.11$ for the bromides. This correlation indicates that the Sb–X bond shortens when its trans Sb · · · X bond lengthens.

Figure 11 shows the relationship between the halogen NQR frequency and the Sb–X bond length. The electric field gradient is in inverse proportion to the third power of the distance from point charges to the resonant nucleus by assuming the point charge model to apply. Figure 12 shows a plot of the NQR frequency against the minus third power of the bond length. An approximately linear relationship exists between them and is expressed by the equations

$$\nu/\mathrm{MHz} = (317/d^3) - 5.68 \quad \text{for the chlorides,}$$

$$\nu/\mathrm{MHz} = (3600/d^3) - 97.0 \quad \text{for the bromides,}$$

where d is the bond length expressed in Ångströms. The NQR frequency is affected to some extent by the interaction with the cation and by other crystal effects. Although at first sight the figure seems to indicate that these factors scarcely affect the frequency, it does not suggest that the contribution from them is very small. The reason for the small sensitivity of the frequency to these factors is that the bond length is also affected by the same factors and their total contributions to the NQR frequency or the bond length have the same sign for all the complexes; for example, the hydrogen bonding between the anion and the cation in these complexes always decreases the ^{81}Br NQR frequency and always lengthens the Sb–Br bond.

Acknowledgement

This work was supported by the Grant-in-Aid for Scientific Research on Priority Area of Organic Unusual Valency No. 04217102 from the Ministry of Education, Science and Culture, Japan.

[1] R. D. Whealy and R. L. Yeakley, J. Inorg. Nucl. Chem. **25,** 365 (1963).
[2] S. W. Hedges and L. H. Bowen, Inorg. Chem. **23,** 1458 (1984)
[3] T. Okuda, N. Tanaka, S. Ichiba, and K. Yamada, Z. Naturforsch. **41a,** 319 (1986).
[4] F. Izumi, M. Mitamo, and Y. Bando, J. Mater. Sci. **19,** 3115 (1984).
[5] T. Okuda, Y. Hashimoto, H. Terao, K. Yamada, and S. Ichiba, J. Mol. Struct. **245,** 103 (1991).
[6] E. Ensinger. W. Schwarz, and A. Schmidt, Z. Naturforsch. **38b**, 149 (1983).
[7] T. Okuda, M. Hiura, E. Koshimizu, H. Ishihara, Y. Kushi, and H. Negita, Chem. Lett. **1982,** 1321.
[8] I. A. Vezzosi, L. P. Barttaglia, and B. Carradi, Inorg. Chim. Acta **89,** 151 (1984).
[9] H. Chihara and N. Nakamura, Advances in Nuclear Quadrupole Resonance, Vol. 4, ed. by J. A. S. Smith, Heyden & Son Ltd., London 1980, p. 1.
[10] D. E. Woessner and H. S. Gutowsky, J. Chem. Phys. **39,** 440 (1963).
[11] Y. Tai, T. Asaji, D. Nakamura, and R. Ikeda, Z. Naturforsch. **45a,** 477 (1990).
[12] T. Okamoto, N. Nakamura, and H. Chihara, Bull Chem. Soc. Japan **52,** 1619 (1979).
[13] H. Ishida, R. Ikeda, and D. Nakamura, Bull. Chem. Soc. Japan **59,** 915 (1986).
[14] T. Okuda, Y. Kinoshita, H. Terao, and K. Yamada, to be reported elsewhere.
[15] L. Pauling, The Nature of the Chemical Bond, Cornell University Press, New York 1960.